Biosensors and Bioelectronics 127 (2019) 85–91

Contents lists available at ScienceDirect

Biosensors and Bioelectronics

journal homepage: www.elsevier.com/locate/bios

Poly-adenine-mediated spherical nucleic acids for strand displacement-based DNA/RNA detection

Lu Wang[a,c,1], Huan Zhang[a,1], Chenguang Wang[a], Yi Xu[a], Jing Su[a], Xiao Wang[a], Xinxin Liu[a], Dezhi Feng[a], Lihua Wang[b], Xiaolei Zuo[d], Jiye Shi[b], Zhilei Ge[b,d,**], Chunhai Fan[b,d], Xianqiang Mi[a,*]

[a] Shanghai Advanced Research Institute, Chinese Academy of Sciences, Shanghai 201220, China
[b] Division of Physical Biology & Bioimaging Center, Shanghai Synchrotron Radiation Facility, Shanghai Institute of Applied Physics, Chinese Academy of Sciences, Shanghai 201800, China
[c] University of Chinese Academy of Sciences, Beijing 100049, China
[d] School of Chemistry and Chemical Engineering, Institute of Molecular Medicine, Renji Hospital, School of Medicine, Shanghai Jiao Tong University, Shanghai 200240, China

ARTICLE INFO

Keywords:
PolyA-AuNPs
DNA strand displacement
DNA/microRNA detection
Bioanalytical chemistry
Multiplexing detection

ABSTRACT

DNA-gold nanoparticles (AuNPs) conjugate is one of the most versatile bionanomaterials for biomedical and clinical diagnosis. However, to finely tune the hybridization ability and precisely control the orientation and conformation of surface-tethered oligonucleotides on AuNPs remains a hurdle. In this work, we developed a poly adenine-mediated spherical nucleic acid (polyA-mediated SNA) strategy by assembling di-block DNA probes on gold nanoparticles (AuNPs) to spatially control interdistance and hybridization ability of oligonucleotides on AuNPs. By modulating length of poly A bound on the SNA with different degrees of constructing, we presented significant improved biosensing performance including high hybridization efficiency, and expanded dynamic range of analytes with more sensitive detection limit. Furthermore, this polyA design could facilitate the programmable detection for DNA in serum environment and simultaneous multicolor detection of three different microRNAs associated with pancreatic carcinoma. The demonstration of the link between modulation of SNA assembly strategy and biodetection capability will increase the development of high performance diagnostic tools for translational biomedicine.

1. Introduction

Advances in materials chemistry and DNA nanotechnology have offered great opportunities for building new biosensors for DNA/RNA detection, which is imperative in biological studies (Chen et al., 2011; Pei et al., 2012a, 2012b; Wang et al., 2015; Yuan et al., 2014; Zeng et al., 2017; F. Zhang et al., 2015; H. Zhang et al., 2015) and clinical diagnosis (Ge et al., 2011; Yan et al., 2014; Yang et al., 2014, 2013; Zhang et al., 2017). Due to the unique chemical and physical properties of gold nanoparticles (AuNPs) (Chai et al., 2010; Howes et al., 2014) and easier access to precisely program DNA nanostructures (Ge et al., 2014; Genot et al., 2011; Rothemund, 2006; F. Zhang et al., 2015; H. Zhang et al., 2015), varies of assays based on DNA-Au NPs probe for DNA/RNA detection were developed (Cutler et al., 2012; Elghanian et al., 1997; Giljohann et al., 2010; Giljohann et al., 2009; Li and Rothberg, 2004; Seferos et al., 2007; Tyagi et al., 1998; Yang et al., 2008; Yao et al., 2015; K. Zhang et al., 2012; Zhang et al., 2012a, 2012b; Zhu et al., 2016). However, despite what has been achieved so far, majority improvement is empirically based on optimization, while rationally design of DNA-AuNPs probes with desirable detection performance remains a hurdle (Pei et al., 2013; Qi et al., 2015; Sheehan and Whitman, 2005; Squires et al., 2008). Herein we developed an approach for the rationally engineering of DNA-Au NPs probes to improve probe performance based on DNA strand displacement reaction (Biala et al., 2015; Chen et al., 2017; P et al., 2015; Srinivas et al., 2013; Zhang and Seelig, 2011; Zhang and Winfree, 2009).

Most DNA/RNA AuNPs biosensors are based on hybridization between complementary sequences (Conde et al., 2015), while target affinity and duplex formation suffer from different constraints (Peterson et al., 2001). For instance, unfavorable probe density lead to

* Corresponding author at: Shanghai Advanced Research Institute, Chinese Academy of Sciences, Shanghai 201220, China.
** Corresponding author.
E-mail addresses: gezhilei@sinap.ac.cn (Z. Ge), mixq@sari.ac.cn (X. Mi).
[1] Equal contributing authors.

https://doi.org/10.1016/j.bios.2018.12.003
Received 21 July 2018; Received in revised form 29 November 2018; Accepted 5 December 2018
Available online 07 December 2018
0956-5663/ © 2018 Elsevier B.V. All rights reserved.

electrostatic repulsion between negatively charged probes and strong steric hindrance (Jacobson et al., 2017); immobilized DNA probe have less configuration freedom (Gong and Levicky, 2008); poor probe conformation and non-specific adsorption restrained hybridization. In light of these difficulties, manipulation of strand interaction and interfacial property is the fundamental way to realize desirable detection performance (Pei et al., 2012a, 2012b; Ye et al., 2017).

Poly adenines (polyA) are consecutive adenine nucleotides that can preferentially bind to the surface of AuNPs with high affinity comparable to Au-S chemistry (Opdahl et al., 2007; Schreiner et al., 2010). With polyA serving as anchor block, the appended recognition block is able to adopt upright conformation and has less non-specific adsorption on AuNPs surface (Pei et al., 2012a, 2012b; Zhu et al., 2016). Furthermore, the surface density of polyA mediated di-block DNA oligonucleotides could be rationally manipulated by varying polyA length (Chen et al., 2017; Zhu et al., 2015). On this basis, we designed a di-block DNA constructed SNA where the recognition block was pre-hybridized with a fluorescence labeled reporter, and the polyA block served as premium anchor block, this design enables tight absorption and leads to effective fluorescence quenching on AuNPs surface when reacts with the DNA/RNA targets. Herein we used 30 nm AuNPs to load di-block DNA and functionalized the SNA with fluorescence labeled reporter DNA, when interrogated by target DNA with different concentration, a relatively sensitive detection limit (10 pM) was obtained. By rationally modulating the polyA length, we realized programmable detection limit on the same SNA substrate. Moreover, this functionalized SNA could detect three pancreatic cancer bio-markers (miRNA155, miRNA196a, miRNA210) simultaneously and exhibited good performance in simulated serum samples, which shows great potential in clinical diagnosis application.

2. Material and methods

2.1. Materials

Gold nanoparticle colloid was purchased from BBI solutions. Trisodium citrate ($C_6H_5Na_3O_7{\cdot}2H_2O$), phosphate, NaCl, $MgCl_2$, KCl were provided by China National Pharmaceutical Group Corporation. All the chemicals were analytical reagents and no further purification before use. Fetal bovine serum (FBS) was provided by Sigma-Aldrich. Milli-Q water was used in this experiment. All of the HPLC purified di-block DNA; target DNA and reporter DNA oligonucleotides were synthesized by Sangon Biological Engineering Co., Ltd in Shanghai. All of the HPLC purified microRNA was synthesized by Invitrogen Company. Sequences of all the DNA and RNA used were shown in Table S1.

2.2. Instruments

JEM-100CX II electron microscope were used to take transmission electron microscopy (TEM) images. UV–Vis spectrometer (U-3010, Hitachi, Tokyo, Japan) were used to record adsorption spectra. Fluorescence spectrometer (FLS900, Edinburgh Instruments Ltd, UK) were employed to collect fluorescence spectra. Analyzer of Zeta Potential Particle and Nano Submicron Particle Size (Delsa™, Beckman Coulter Inc., United States) were used to measure hydrodynamic diameters. Digital pH-meter (FE20, Mettler-Toledo, China) were used for pH value measurement.

2.3. Preparation of polyA-AuNPs

PolyA mediated SNA was constructed using the pH-assisted method (K. Zhang et al., 2012; Zhang et al., 2012a, 2012b). First, di-block DNA was hybridized with reporter DNA by annealing in PCR machine. The hybridized di-block probe was add to AuNPs (0.5 nM) with the ratio of 1000:1. Then they were incubated the mixture for 10 min in room temperature. Secondly, add in 500 mM, pH = 3 citrate HCl buffer to the mixture and final concentration is 10 mM. The sample was mixed slightly and kept in room temperature for 10 min. Then, adjusted the pH of solution back to neutral by using 200 mM, pH = 7.6 PB buffer (9 μl buffer for 50 μl mixed solution) and incubated at room temperature for 5–10 min. We centrifugated the mixed solution at 8000 rpm, 4 °C and washed it three times to remove un-assembled di-block probe by using 10 mM PB buffer (pH = 7.6). The SNA were dispersed in pH = 7.6, 1xPBS buffer with final concentration of 0.15 nM for further experiments (concentration was calculated by emission peak value at 530 nm, $\varepsilon = 2.7 \times 10^8\ \mathrm{L\,mol^{-1}\,cm^{-1}}$).

2.4. Quantitation of di-block probes loaded on AuNP

We quantified the amounts of di-block probes loaded on AuNPs following the protocol (Alivisatos et al., 1996). The mercaptoethanol with final concentration of 20 mM were added into SNA and incubated overnight at room temperature with shaking. The fluorophore (FAM)-labeled DNA left the surface of AuNPs. We separated the released probes by centrifugation and measured fluorescence intensity at 520 nm with a fluorescence spectrometer (excitation wavelength: 494 nm). The standard linear calibration curves was depicted with different concentrations of fluorescence DNA in the same ME concentration, buffer pH and ionic strength (Fig. S2). By using standard linear calibration curves, fluorescence intensity convert to molar concentration of released DNA.

2.5. Toehold length regulation for di-block probe

We designed a series of reporter DNA with different nucleotide number to hybridize with the di-block DNA. Di-block probes hybridized with different reporter had 1nt, 3nt, 5nt, 7nt, 9nt, 11nt toeholds respectively and labeled as T-1, T-3, T-5, T-7, T-9, T-11. SNA (0.15 nM) were constructed by the above assay. Targets were added and the final concentration was 5 nM. After incubation, the fluorescence labeled reporters were separated by centrifugation at 8000 rpm, 4 °C. The fluorescence intensity of FAM-labeled reporter was measured at 520 nm with excitation wavelength at 494 nm. SNR were calculated using target signal divided by noise signal and all the results were calculated by three repeated experiments.

2.6. PolyA length regulation for di-block probe

Three different di-block probes with 30As, 40As and 50As were pre-hybridized with FAM labeled reporter DNA. SNA were constructed by the above assay with the final concentration of 0.15 nM. Targets with different concentrations (0, 0.01, 0.05, 0.1, 0.5, 1, 5, 10, 50, 100, and 200 nM) were added. After incubation, the fluorescence labeled reporter were separated by centrifugation at 8000 rmp, 4 °C. The fluorescence intensity of FAM-labeled reporter was excited at 494 nm and measured at 520 nm. The results were calculated by three repeated experiments. Colloidal stability experiments for A30 SNA, A40 SNA and A50 SNA were shown in Figs. S3 and S4.

2.7. Specificity of DNA detection

Target DNA and non-target DNA were added into 200 μL hybridization buffer (0.15 nM SNA) with the final concentration of 5 nM (target DNA) and 50 nM (non-target DNAs). After incubation, the fluorescence labeled reporter were obtained by centrifugation at 8000 rpm, 4 °C. The fluorescence intensity of FAM-labeled reporter was measured at 520 nm (excitation wavelength: 494 nm). The results were calculated by three repeated experiments.

2.8. microRNA detection of SNA

Three di-block probes were designed with different complementary

recognition blocks and hybridized with three different reporters labeled with Cy5, ROX and FAM for microRNA155, microRNA196a and microRNA210, respectively. These di-block probes were mixed with 1:1:1 ratio to construct SNA (0.15 nM) by the above assay. Then three target microRNAs with the final concentration of 10 nM were added together. After incubation, the fluorescence labeled reporter were separated by centrifugation at 8000 rpm, 4 °C in supernatant. The fluorescence intensity of FAM-labeled reporter was excited at 494 nm and measured at 520 nm, ROX-labeled reporter were excited at 588 nm and measured at 608 nm, cy5-labeled reporter were excited at 647 nm and measured at 670 nm. The results were calculated by three repeated experiments.

2.9. Target DNA detection in fetal bovine serum

For the target detection in diluted FBS, we diluted 100 μL of FBS with 900 μL PBS buffer (pH 7.6, 100 mM). Then DNA target were added to the diluted FBS (10%) with final concentration of 10 nM. We used SNA to detected DNA target in diluted FBS and recorded the fluorescence. The results were calculated by three repeated experiments.

3. Results and discussion

3.1. Construction of SNA

We constructed SNA with di-block probes based on strong absorption of polyA to AuNPs in low pH citric sodium. The recognition block was hybridized with a FAM labeled reporter, and the polyA block served as anchor probe (shown in Scheme 1). The whole assembly process of poly A-dsDNA and AuNPs could be completed in a few minutes following the rapid assembly protocol, and lead to a stoichiometric control of reporter DNA and polyA-DNA, which made the re-hybridization between reporter DNA and polyA-DNA more easily than step-by-step processing at pH 7 conditions. Due to the high affinity of polyA to AuNPs, we spatially controlled DNA recognition domain assembled on AuNPs by varying length of polyA block. Previous reports have illustrated the effect of DNA sequence for non-thiolated DNA adsorption by AuNPs systematically (Huang et al., 2016; Liu and Liu, 2017; K. Zhang et al., 2012; Zhang et al., 2012a; 2012b, 2013).

Surface density of oligonucleotide on AuNPs was quantified by using the displacement-based fluorescence method. The surface density decreased along with the length increase of the polyA block (Fig. 1a), which indicated that the inter-strand spacing on AuNPs increased. In this case, we modified the AuNPs with polyA 30, polyA 40 and polyA 50 di-block DNA probes, respectively. Each 30 nm AuNP carried about 39 di-block DNAs for polyA 30 di-block probes (A30 DPs), 27 di-block DNAs for polyA 40 di-block probes (A40 DPs), and 23 polyA 50 di-block probes (A50 DPs) shown in Figs. 1b and S2.

This observation is consisted with previous reported phenomenon (Pei et al., 2012a, 2012b). TEM images (Fig. 1c) presented that both the naked AuNPs and SNA were uniformly distributed, which suggested the AuNPs were well protected during the assembly process. The maximum absorption peak shifted from 525 nm to 530 nm in UV–Vis absorption spectra (Fig. 1d) after assembly of oligonucleotides, which confirmed the successful modification of di-block probes on AuNPs. The dynamic light scattering (DLS) analysis data proved that the hydrodynamic diameters increased from 10 nm to 12.6 nm after covered by di-block probes, and the final diameter varied with the polyA length of di-block DNA (Fig. S1).

Previous report have demonstrated that polyA can replace the thiol group by strongly binding to AuNPs and competitively displacing other base combinations. Given the high-adsorption affinity of polyA on AuNPs, we varied the length of polyA blocks to spatially control the assembly of oligonucleotides on AuNPs.

Since the surface density decreased along with the length increase of the polyA block (Fig. 1a), the increase of inter-strand spacing was obtained on AuNPs. Interestingly, interestingly, when the density was normalized in terms of A bases, nearly the same amount was obtained for all diblock oligonucleotides. This nice coincidence suggests that all A bases in the polyA block, independent of the length, are completely adsorbed on AuNPs to enable full surface coverage.

3.2. Toehold length modulation of SNA

As shown in Scheme 1, the di-block DNA was hybridized with FAM labeled reporter and spared a toehold region, which served as anchor for target sequences and initiated strand displacement reaction. Previous reports had shown that the toehold length strongly influenced strand interaction and the rate of strand displacement reaction (Zhang and Winfree, 2009). Hence, we engineered SNA with 1nt, 3nt, 5nt, 7nt, 9nt, 11nt toeholds respectively and investigated the effect of toehold length on SNA performance by detecting the same target of 5 nM. The signal noise ratio (SNR) was calculated by recording the fluorescence intensity (Fig. S8). The results showed that each SNR increased to a peak value and then decreased with the increase of toehold length. This tendency was confirmed in SNA with 30As, 40As and 50As. SNR improved 4.08 folds in A30 SNA with 7 nt toehold, 12.22 folds in A40 SNA with 5 nt toehold and 9.48 folds in A50 SNA with 7 nt toehold in this experiment. The maximum SNR value was obtained with 7 nt or 5 nt toeholds.

The tendency could be ascribed to the thermodynamics of DNA displacement reaction (Zhang and Winfree, 2009). When the toehold is less than 5nt, the DNA displacement reaction could not initiate effectively, while the toehold is more than 7 nt, the reaction between di-block DNA and reporter DNA will be reduced significantly which leads to a higher background signal (Wong et al., 2005). The results indicated that toehold length could regulate detection ability of polyA-AuNP effectively.

3.3. Poly-A length modulation of SNA (sensitivity and specificity of DNA detection)

Previous reports have shown that polyA-mediated SNA with different polyA lengths displayed different hybridization efficiency (Pei et al., 2012a, 2012b). The poly-A length could affect the thermodynamics and kinetics of DNA hybridization on gold nanoparticle. We

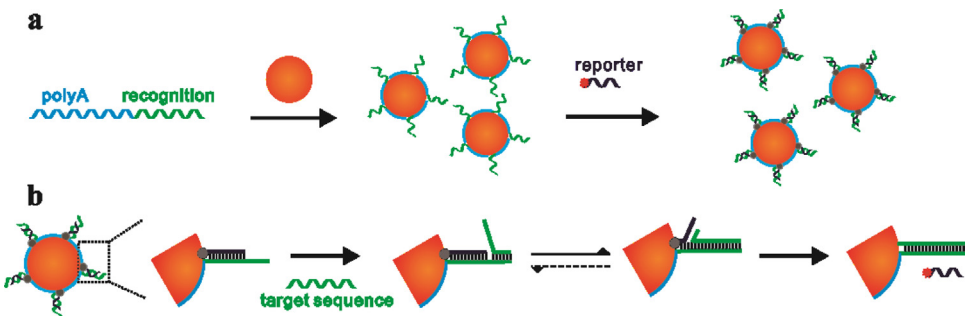

Scheme 1. Illustration of the assembling of polyA-AuNPs. a) Constructing of polyA-AuNPs. b) Recognition block of DNA, hybridized with FAM labeled reporter in advance and fluorescence quenched. The toehold served as anchor for target sequences and initiated strand displacement reaction when reacted with target DNA. After branch migration, FAM labeled reporter was displaced and fluorescence signal could be detected.

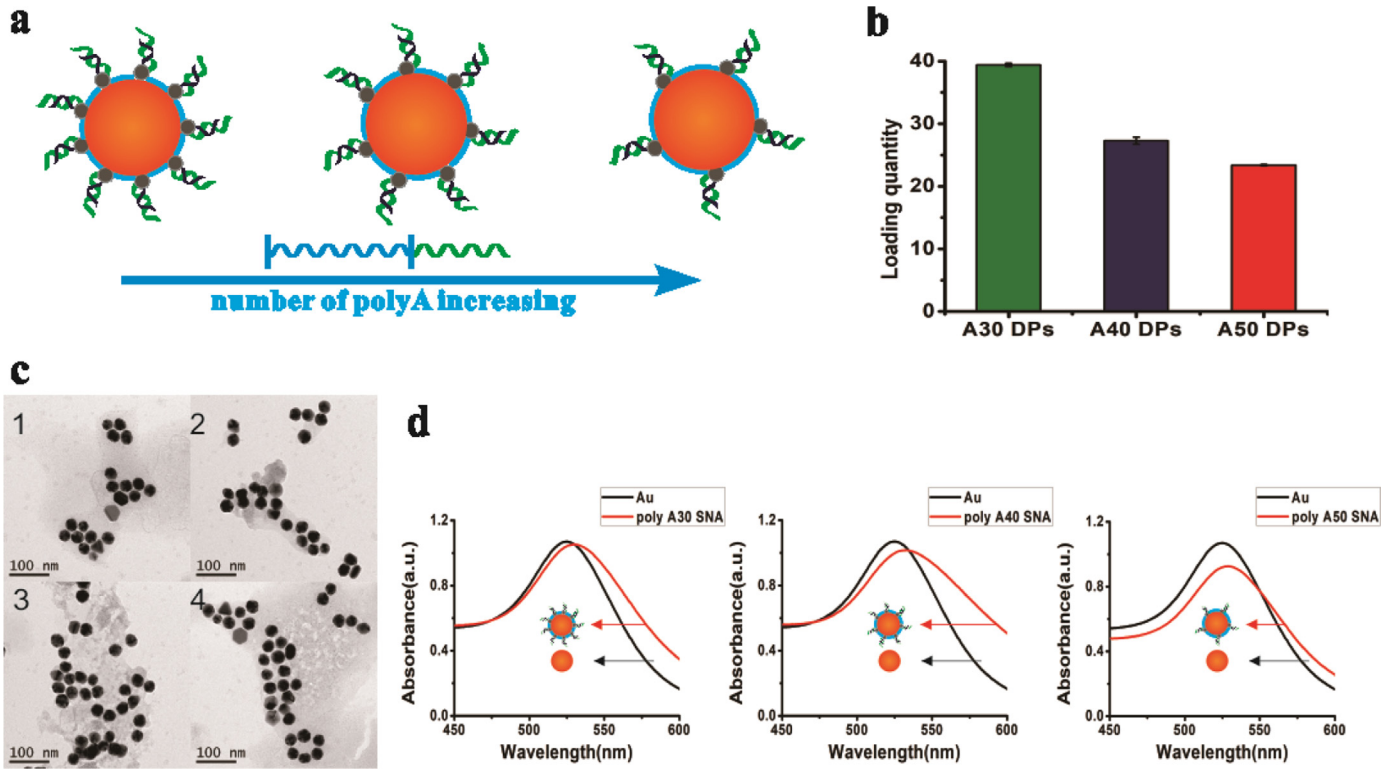

Fig. 1. (a)Schematic for spatial control on AuNPs by varying the length of polyA blocks. (b) Loading quantity of assembled di-block probes on SNA (DPs means di-block probes). (c) TEM images: c1) AuNP, c2) poly A30 SNA, c3) poly A40 SNA, c4) poly A50 SNA. (d) UV–Vis absorption spectra of naked AuNPs and corresponding SNA.

prepared a series of SNA with A30, A40 and A50 as anchor blocks and optimized 7nt toehold for recognition block. To assess the sensitivity of SNA, we employed them to detect target concentration ranging from 10 pM to 200 nM.

By recording the fluorescence intensity, the concentration-fluorescence intensity curve was depicted in Fig. S5. It showed that the fluorescence intensity increased linearly with target concentration until to a plateau. The linear range of A30 SNA, A40 SNA and A50 SNA were 0.1–10 nM, 0.05–10 nM and 0.01–5 nM, respectively (Fig. S5 inserted). Previous reports (Ma et al., 2015; Ma et al., 2016) have demonstrated that SNA based DNA detection could facilitate 2.5 nM sensitivity, meanwhile in our system, the detection limit of poly A30 SNA, poly A40 SNA and poly A50 SNA were 100 pM, 50 pM and 10 pM, respectively, which had greatly improved the sensitivity of SNA based nucleic acids biosensor system by 2 orders of magnitude.

As shown in Fig. 2b, the detection limit differed with the poly-A lengths. Better sensitivity was obtained on the polyA 50 DNA-AuNPs. When assembled with polyA strands, the probe density in A50 SNA is much lower than A30 SNA, which made the hybridization process of target DNA and probes on SNAs more accessible and efficient. The lateral spacing and surface density of DNA on AuNPs could be systematically modulated by adjusting the length of polyA block. Based on our previous reports (Pei et al., 2012a, 2012b; Zhu et al., 2016), the longer polyA lengths was, the thermodynamic properties were more similar to that of duplex in solution than on surface. Meanwhile fast hybridization rate was observed on the di-block DNA-AuNPs and was also increased along with the length of polyA block (Fig. S7). Thus we concluded from the above results that by changing length of polyA block, one could adjust the bio-sensing capability of SNA effectively. Since the limits of detection based on this SNA system were influenced by the anchor block length, with this unique feature we were able to construct a rational design biosensor system based on polyA SNA with expanded dynamic range to monitor disease-associated nucleic acids at different level, such as cancer-related genes, which differed with many orders of magnitude in patient (Ludwig and Weinstein, 2005).

Furthermore, we investigated the specificity of SNA with different polyA lengths. Three different DNA strands were tested, including the complementary target DNA and two random DNA strands (seq. 1 and seq. 2) (Sequences were shown in Table S1). As show in Fig. 2c, no obvious fluorescence intensity increase of random DNA were observed compared with the target DNA, even the concentration of random DNA was 10 times higher than target DNA (50 nM/5 nM).

3.4. Multiplexed detection of tumor markers

The ability to detect multiple disease-related targets from a single biological sample in a quick and reliable manner is of high importance in diagnosing and monitoring disease. Due to the complexity of biological system, especially the human body, single biomarker alone is not effective enough for accurate diagnosis (Laing et al., 2016). MicroRNA can be used as a bio-marker for screening and detecting tumor in early stage (Ambros, 2004; Ge et al., 2014; Li et al., 2012; Song et al., 2012; Zeng et al., 2017), simultaneous multicolor detection helps for improving accuracy of early cancer detection (Qiao et al., 2011; Tyagi et al., 1998). For further detection of microRNA with extremely low concentration in human fluids (Chen et al., 2008), we employed poly A50 SNA for multicolor detection. The multiplexing testing of SNAs is attributed to their robust assembly of DNA. Three pancreatic cancer bio-markers (microRNA 155, microRNA 196a, microRNA 210) were chosen as targets. To facilitate the simultaneous detection of tumor markers by SNA, co-assembly strategy was employed to construct multicolor SNAs in one polyA-AuNPs system, where reporters were labeled with Cy5, ROX and FAM respectively. When adding three targets in this detection platform, SNA responded to each target specifically, and 10 nM targets could be observed without interfacing with each other (Fig. 3). Here, we detected a panel of three pancreatic carcinoma (PC) associated miRNAs (miRNA155, miRNA196a and miRNA210) simultaneously which have been reported to be over

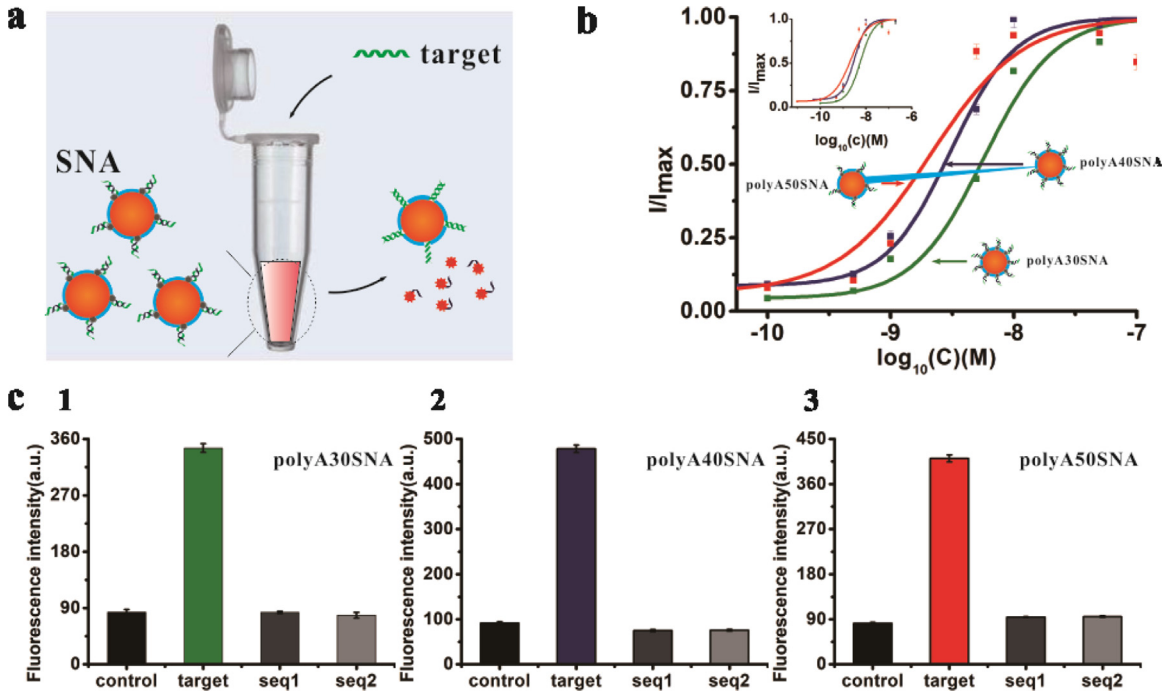

Fig. 2. a) DNA Detection process of SNA. b) Comparison of the detection limit and dynamic range of three SNAs with different polyA lengths. c) Fluorescence signal of target DNA (5 nM) and random DNA (50 nM): (c1) poly A30 SNA (c2) poly A40 SNA (c3) poly A50 SNA. Each experiments were conducted three times.

expressed in pancreatic ductal adenocarcinoma. Besides, we have labeled three miRNA targets with three fluorescence dyes with un-overlapped fluorescence spectra, the cross reactions could be excluded from our measurements. This result proved that the SNA could distinguish specific microRNA targets effectively and realize synchronous multicolor detection, which holded great promise for developing new generations of point of care testing techniques in clinical applications.

3.5. DNA detection in simulated serum

To explore the potential clinical use of di-block probes modified SNA, we interrogated it in complex bio-sample with 10% fetal bovine serum. Despite the interference of other components in the simulated biological fluids (e.g. proteins), our preliminary results still showed that SNA specifically responded to 10 nM target sequences and displayed a

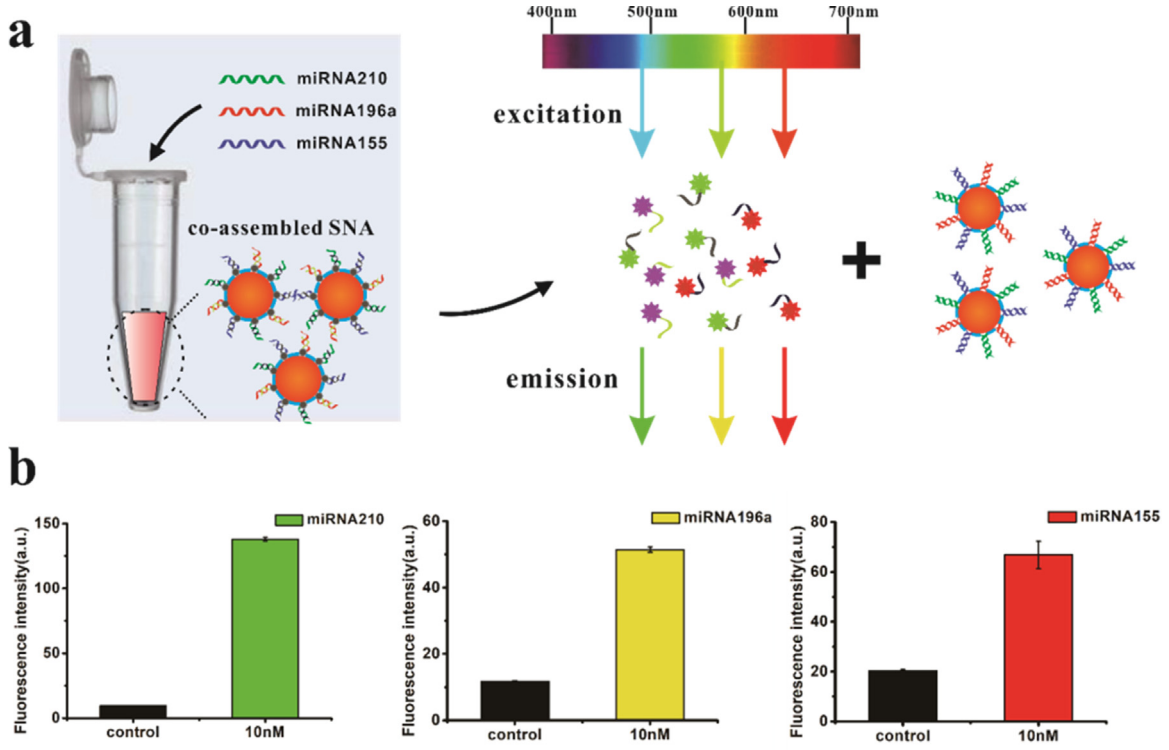

Fig. 3. a) Schematic showing the simultaneous multicolor detection of three microRNAs with polyA50 SNA. b) Three different microRNAs with a concentration of 10 nM were tested in the same tube. Each experiments were conducted three times.

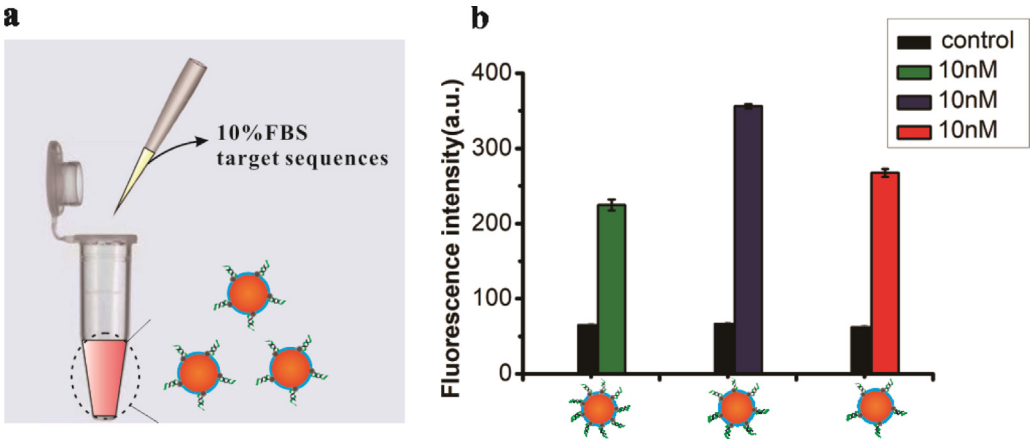

Fig. 4. a) SNA used for simulated serum detection. b) SNA with different anchor block lengths were tested(A30, A40, A50). Each experiments were conducted three times.

significant fluorescence signal increase (Fig. 4). As shown in Fig. 4a, we chose 10 nM DNA target in 10% FBS solution, and the fluorescence generated by the incubation with polyA-AuNP complex was monitored in Fig. 4b. Obvious fluorescence intensity increase was observed in A30, A40, A50 systems, which indicated the detection of target DNA. The capability to detect the corresponding target in complex media made polyA-AuNPs approach a very promising method to fulfill target detection under complicated condition and exhibited great potential for clinical diagnosis.

4. Conclusions

In summary, we developed a poly adenine-mediated spherical nucleic acid (SNA) with programmable detection ability by modulating toehold and poly A length of di-block DNA for DNA/RNA detection. By modulating length of poly A di-block DNA, detection limit of SNA decreased 2 orders compared with previous reported SNA system. Furthermore, we realized simultaneous multicolor detection of three different pancreatic cancer related microRNAs (miRNA-155, miRNA-196a, miRNA210) by co-assembly strategy. Given all these advantages, we envision that this novel SNA with programmable detection ability have great potential for clinical diagnosis.

Acknowledgements

We are appreciated for support from the National Key Research and Development Program of China (Grant 2016YFC0100600), National Key Technology Research and Development Program of the Ministry of Science and Technology of China (Grant 2015BAI02B02, 2013CB932803, 2013CB933802, 2016YFA0201200), the National Natural Science Foundation of China (Grant 21605153, 21329501, 21227804), Science and Technology Service Network Initiative, the Chinese Academy of Sciences (Grant KFJ-EW-STS-140, KFJ-EW-STS096, QYZDJ-SSW-SLH031), the Ministry of Science and Technology of China (2013CB932803, 2013CB933802, 2016YFA0201200) and Shanghai Municipal Science and Technology Commission (Grant 15441905000, 16DZ1930700).

Declaration of interest statement

The authors declare no competing interests.

Appendix A. Supporting information

Supplementary data associated with this article can be found in the online version at doi:10.1016/j.bios.2018.12.003.

References

Alivisatos, A.P., Johnsson, K.P., Peng, X., Wilson, T.E., Loweth Jr, C.J., Bruchez, M.P., Schultz, P.G., 1996. Nature 382 (6592), 609–611.
Ambros, V., 2004. Nature 431 (7006), 350–355.
Biala, K., Sedova, A., Flechsig, G.U., 2015. ACS Appl. Mater. Interfaces 7, 19948–19959.
Chai, F., Wang, C.A., Wang, T.T., Li, L., Su, Z.M., 2010. ACS Appl. Mater. Interfaces 2, 1466–1470.
Chen, L.Z., Chao, J., Qu, X.M., Zhang, H.B., Zhu, D., Su, S., Aldalbahi, A., Wang, L.H., Pei, H., 2017. ACS Appl. Mater. Interfaces 9 (9), 8014–8020.
Chen, P., Pan, D., Fan, C.H., Chen, J.H., Huang, K., Wang, D.F., Zhang, H.L., Li, Y., Feng, G.Y., Liang, P.J., He, L., Shi, Y.Y., 2011. Nat. Nanotechnol. 6, 639–644.
Chen, X., Ba, Y., Ma, L., Cai, X., Yin, Y., Wang, K., Guo, J., Zhang, Y., Chen, J., Guo, X., 2008. Cell Res. 18 (10), 997–1006.
Conde, J., Edelman, E.R., Artzi, N., 2015. Adv. Drug Del. Rev. 81, 169–183.
Cutler, J.I., Auyeung, E., Mirkin, C.A., 2012. J. Am. Chem. Soc. 134 (3), 1376–1391.
Elghanian, R., Storhoff, J.J., Mucic, R.C., Letsinger, R.L., Mirkin, C.A., 1997. Science 277 (5329), 1078–1081.
Ge, Z., Lin, M., Wang, P., Pei, H., Yan, J., Shi, J., Huang, Q., He, D., Fan, C., Zuo, X., 2014. Anal. Chem. 86 (4), 2124–2130.
Ge, Z.L., Pei, H., Wang, L.H., Song, S.P., Fan, C.H., 2011. Sci. China Chem. 54, 1273–1276.
Genot, A.J., Zhang, D.Y., Bath, J., Turberfield, A.J., 2011. J. Am. Chem. Soc. 133, 2177–2182.
Giljohann, D.A., Seferos, D.S., Daniel, W.L., Massich, M.D., Patel, P.C., Mirkin, C.A., 2010. Angew. Chem. Int. Ed. 49 (19), 3280–3294.
Giljohann, D.A., Seferos, D.S., Prigodich, A.E., Patel, P.C., Mirkin, C.A., 2009. J. Am. Chem. Soc. 131 (6), 2072–2073.
Gong, P., Levicky, R., 2008. Proc. Natl. Acad. Sci. USA 105, 5301–5306.
Howes, P.D., Chandrawati, R., Stevens, M.M., 2014. Science 346 (6205), 53–63.
Huang, Z., Liu, B., Liu, J., 2016. Langmuir 32 (45), 11986–11992.
Jacobson, D.R., McIntosh, D.B., Stevens, M.J., Rubinstein, M., Saleh, O.A., 2017. Proc. Natl. Acad. Sci. USA 114, 5095–5100.
Laing, S., Gracie, K., Faulds, K., 2016. Chem. Soc. Rev. 45 (7), 1901–1918.
Li, H.X., Rothberg, L.J., 2004. Anal. Chem. 76 (18), 5414–5417.
Li, N., Chang, C.Y., Pan, W., Tang, B., 2012. Angew. Chem. Int. Ed. 51 (44), 10922 (10922).
Liu, B., Liu, J., 2017. Anal. Methods 9 (18), 2633–2643.
Ludwig, J.A., Weinstein, J.N., 2005. Nat. Rev. Cancer 5 (11), 845–856.
Ma, J.L., Yin, B.C., Le, H.N., Ye, B.C., 2015. ACS Appl. Mater. Interfaces 7 (23), 12856–12863.
Ma, X.Z., Wang, M., Chen, C., Isbell, M.A., Wang, R., Liu, D.S., Yang, Z.Q., 2016. Sci. China Chem. 59 (6), 765–769.
Opdahl, A., Petrovykh, D.Y., Kimura-Suda, H., Tarlov, M.J., Whitman, L.J., 2007. Proc. Natl. Acad. Sci. USA 104 (1), 9–14.
Šulc, P., Ouldridge, T.E., Romano, F., Doye, J.P., Louis, A.A., 2015. Biophys. J. 108, 1238–1247.
Pei, H., Li, F., Wan, Y., Wei, M., Liu, H.J., Su, Y., Chen, N., Huang, Q., Fan, C.H., 2012a. J. Am. Chem. Soc. 134 (29), 11876–11879.
Pei, H., Liang, L., Yao, G., Li, J., Huang, Q., Fan, C., 2012b. Angew. Chem. Int. Ed. 51 (36), 9020–9024.
Pei, H., Zuo, X.L., Pan, D., Shi, J.Y., Huang, Q., Fan, C.H., 2013. Npg Asia Mater. 5, e51–e60.
Peterson, A.W., Heaton, R.J., Georgiadis, R.M., 2001. Nucleic Acids Res. 29, 5163–5168.
Qi, H., Huang, G.Y., Han, Y.L., Zhang, X.H., Li, Y.H., Pingguan-Murphy, B., Lu, T.J., Xu, F., Wang, L., 2015. Tissue Eng. Part B Rev. 21, 288–297.
Qiao, G.M., Gao, Y., Li, N., Yu, Z.Z., Zhuo, L.H., Tang, B., 2011. Chem. Eur. J. 17 (40), 11210–11215.
Rothemund, P.W.K., 2006. Nature 440, 297–302.
Schreiner, S.M., Shudy, D.F., Hatch, A.L., Opdahl, A., Whitman, L.J., Petrovykh, D.Y.,

2010. Anal. Chem. 82 (7), 2803–2810.
Seferos, D.S., Giljohann, D.A., Hill, H.D., Prigodich, A.E., Mirkin, C.A., 2007. J. Am. Chem. Soc. 129 (50), 15477–15479.
Sheehan, P.E., Whitman, L.J., 2005. Nano Lett. 5, 803–807.
Song, M., Pan, K., Su, H., Zhang, L., Ma, J., Li, J., Yuasa, Y., Kang, D., Yong, S.K., You, W., 2012. PLoS One 7 (3), e33608.
Squires, T.M., Messinger, R.J., Manalis, S.R., 2008. Nat. Biotechnol. 26 (4), 417–426.
Srinivas, N., Ouldridge, T.E., Sulc, P., Schaeffer, J.M., Yurke, B., Louis, A.A., Doye, J.P.K., Winfree, E., 2013. Nucleic Acids Res. 41, 10641–10658.
Tyagi, S., Bratu, D.P., Kramer, F.R., 1998. Nat. Biotechnol. 16 (1), 49–53.
Wang, C.G., Zhang, H., Zeng, D.D., Sun, W.L., Zhang, H.L., Aldalbahi, A., Wang, Y.S., San, L.L., Fan, C.H., Zuo, X.L., Mi, X.Q., 2015. Nanoscale 7 (38), 15822–15829.
Wong, E.L., Chow, E., Gooding, J.J., 2005. Langmuir 21, 6957–6965.
Yan, J., Hu, C., Wang, P., Liu, R., Zuo, X., Liu, X., Song, S., Fan, C., He, D., Sun, G., 2014. ACS Appl. Mater. Interfaces 6 (22), 20372–20377.
Yang, F., Zuo, X.L., Li, Z.H., Deng, W.P., Shi, J.Y., Zhang, G.J., Huang, Q., Song, S.P., Fan, C.H., 2014. Adv. Mater. 26 (27), 4671–4676.
Yang, J., Shen, L.J., Ma, J.J., Schlaberg, H.I., Liu, S., Xu, J., Zhang, C., 2013. ACS Appl. Mater. Interfaces 5, 5392–5396.
Yang, R.H., Jin, J.Y., Chen, Y., Shao, N., Kang, H.Z., Xiao, Z., Tang, Z.W., Wu, Y.R., Zhu, Z., Tan, W.H., 2008. J. Am. Chem. Soc. 130 (26), 8351–8358.
Yao, G.B., Li, J., Chao, J., Pei, H., Liu, H.J., Zhao, Y., Shi, J.Y., Huang, Q., Wang, L.H., Huang, W., Fan, C.H., 2015. Angew. Chem. Int. Ed. 54 (10), 2966–2969.
Ye, D.K., Zuo, X.L., Fan, C.H., 2017. Prog. Chem. 29, 36–46.
Yuan, Z., Zhou, Y.Y., Gao, S.X., Cheng, Y.Q., Li, Z.P., 2014. ACS Appl. Mater. Interfaces 6, 6181–6185.
Zeng, D., Wang, Z., Meng, Z., Wang, P., San, L., Wang, W., Aldalbahi, A., Li, L., Shen, J., Mi, X., 2017. ACS Appl. Mater. Interfaces 9 (28), 24118–24125.
Zhang, D.Y., Seelig, G., 2011. Nat. Chem. 3 (2), 103–113.
Zhang, D.Y., Winfree, E., 2009. J. Am. Chem. Soc. 131, 17303–17314.
Zhang, F., Jiang, S., Wu, S., Li, Y., Mao, C., Liu, Y., Yan, H., 2015a. Nat. Nanotechnol. 10 (9), 779–784.
Zhang, H., Chao, J., Pan, D., Liu, H., Qiang, Y., Liu, K., Cui, C., Chen, J., Huang, Q., Hu, J., 2017. Nat. Commun. 8, 14738.
Zhang, H., Wang, Y., Zhao, D., Zeng, D., Xia, J., Aldalbahi, A., Wang, C., San, L., Fan, C., Zuo, X., Mi, X., 2015b. ACS Appl. Mater. Interfaces 7 (30), 16152–16156.
Zhang, K., Hao, L., Hurst, S.J., Mirkin, C.A., 2012a. J. Am. Chem. Soc. 134 (40), 16488–16491.
Zhang, X., Liu, B., Dave, N., Servos, M.R., Liu, J., 2012a. Langmuir 28 (49), 17053–17060.
Zhang, X., Liu, B., Servos, M.R., Liu, J., 2013. Langmuir 29 (20), 6091–6098.
Zhang, X., Servos, M.R., Liu, J.W., 2012b. J. Am. Chem. Soc. 134 (17), 7266–7269.
Zhu, D., Pei, H., Chao, J., Su, S., Aldalbahi, A., Rahaman, M., Wang, L.H., Wang, L.H., Huang, W., Fan, C.H., Zuo, X.L., 2015. Nanoscale 7, 18671–18676.
Zhu, D., Song, P., Shen, J.W., Su, S., Chao, J., Aldalbahi, A., Zhou, Z., Song, S.P., Fan, C.H., Zuo, X.L., Tian, Y., Wang, L.H., Pei, H., 2016. Anal. Chem. 88 (9), 4949–4954.